New optimized digital filters for sine, co-sine, J_0 and J_1 Hankel transforms

Luiz Rijo and Frayzer Lima de Almeida UFPA, Brazil

Abstract

Fourier and Hankel transforms play a fundamental role on the analysis of electrical and electromagnetic geophysical data. There are many efficient numerical algorithms for evaluating Fourier and Hankel transforms. However, for electrical geophysics the digital linear filter algorithm seems to be the most appropriated due to its simplicity and efficiency. In this paper we present a new set of optimized filters for Sine, Co-sine and J_0 and J_1 Hankel transforms. Through many examples of geophysical problems we attested the high performance of these new optimized filters.

Introduction

Fourier and Hankel transforms are widely used in the theory of the electrical and electromagnetic geophysical methods. This can be attested from the extensive pertinent literature: Ghosh (1971), Koefoed et al. (1972), Verma and Koefoed (1973), Das and Ghosh (1974), O'Neill (1975), Verma (1977), Koefoed and Dirks (1979), Johansen and Sorensen (1979), Anderson (1979), Guptasarma (1982), Nissen and Enmark (1986), Rijo (1988)., Mohsen and Hashish (1994), Rijo (1996) .
Ghosh (1971) and Koefoed (1972) were the first to apply the digital linear filter theory to evaluate numerically the Stafanesco integral (Hankel transform) associated with Sclumberger electrical soundings. From these pioneer works theirs algorithm was improved to cover many electrical geophysics techniques.
In this paper we present a set of new optimized filters for Sine, Co-sine and J_0 and J_1 Hankel transforms calculated with an automatic scheme based on Guptasarma and Singh algorithm (1997)

The digital filters

The sine, co-sine and J_0 and J_1 Hankel transforms can be represented by the integral

$$F\left(x\right)=\int_0^\infty f\left(\lambda\right)g\left(\lambda x\right)d\lambda, \qquad (1)$$

where the function g is any of the four functions: sine, co-sine, J_0 and J_1.
With a simple transformation of variable this integral can be replaced by

$$xF\left(x\right)=\int_0^\infty f\left(\lambda/x\right)g\left(\lambda\right)d\lambda.$$

Now, substituting x for e^p and λ for e^λ, we obtain the convolution integral

$$xF\left(x\right)=\int_{-\infty}^\infty f\left(e^{-(p-s)}\right)e^s g\left(e^s\right)d\lambda\,,$$

where $f\left(e^{-(p-s)}\right)$ and $F\left(x\right)$ are, respectively, the input and output functions and $e^s g\left(e^s\right)$ the *filter function*. The numerical approximation of this convolution integral takes the form:

$$xF\left(x\right)=\sum_{n=1}^N f\left(e^{-(\ln x-\eta_n)}\right)W_n \qquad . \qquad (2)$$

Many algorithms -- Ghosh (1971), Koefoed and Dirks (1979), Johansen and Sorensen (1979), Anderson (1979), Guptasarma (1982), Mohsen and Hashish (1994), and Frayzer (2002) -- have been proposed for evaluating the abscissas η_n and the filter coefficients W_n of the convolution (2). The filters shown in Tables I, II, II and IV were calculated by an automatic process which improves substantially the scheme proposed by Guptasarma and Singh (1982). Both strategies are based on the Wiener-Hopf least squared method for filter designing, Koefoed and Dirks (1979). The algorithm by Guptasarma and Singh uses a graphical strategy to help to select the optimal values of η_n and W_n given by Wiener-Hopf. Besides be very laborious the real drawback of Guptasarma and Singh scheme is to guess, a priori, the first abscissa, known as Koefoed shift (Koefoed,1972; Rijo,1998). In the new scheme, the Koefoed shift is calculated automatically and therefore there is not necessity to guess the first abscissa of the filter.

Example 1:

In this example we compare the calculated against the exact values of the mutual coupling ratio of the vertical component of the magnetic field at 1000 m from an infinite line-source on an homogeneous 100 half-space.

$$Z/Z_0 = 2\bar{x}\int_0^\infty \frac{g}{g+\bar{u}}\sin(g\bar{x})\,dg,$$

$$Z/Z_0 = -\frac{2i}{\bar{x}}\left\{1-\bar{x}(1+i)K_1\left[\bar{x}(1+i)\right]-i\bar{x}^2K_0\left[\bar{x}(1+i)\right]\right\}$$

where K_0 and K_1 are the second kind modified Bessel function of order 0 and 1. The normalized distance $\bar{x}=x/\delta$, where $\delta=\sqrt{T/(\pi\mu_0\sigma)}$ is the skin depth and T is the period.

The Figure 1 shows the perfect adjustment between the calculated – formula 2 with sine filter of Table II -- and the exact values of the mutual coupling ratio of the vertical component of the magnetic fields.

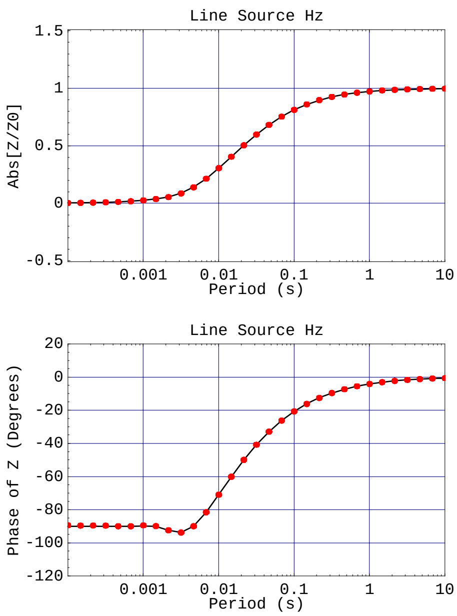

Figura 1. The red dots represent the calculated values and the black curve the exact mutual coupling ratio.

Example 2:

In this example we compare the calculated against the exact values of the mutual coupling ratio of the horizontal component of the magnetic field at 1000 m from an infinite line-source on an homogeneous 100   half-space.

$$Z/Z_0 = -2\bar{x}\int_0^\infty \frac{u}{g+\bar{u}}\cos(g\bar{x})\,dg,$$

$$Z/Z_0 = 2\bar{x}(1+i)\left\{\frac{1}{3}+\frac{\pi}{2}\left[\frac{J_2\left[-\bar{x}(1+i)\right]}{\bar{x}(1+i)}+\frac{\mathbf{H}_2\left[-\bar{x}(1-i)\right]}{\bar{x}(1-i)}\right]\right\}$$

where J_2 is the Bessel and $\mathbf{H}_2$ is the Struve functions of order 2. The normalized distance $\bar{x}=x/\delta$, where $\delta=\sqrt{T/(\pi\mu_0\sigma)}$ is the skin depth and T is the period.

The Figure 2 shows the perfect adjustment between the calculated – formula 2 with co-sine filter of Table I -- and the exact values of the mutual coupling ratio of the horizontal component of the magnetic fields

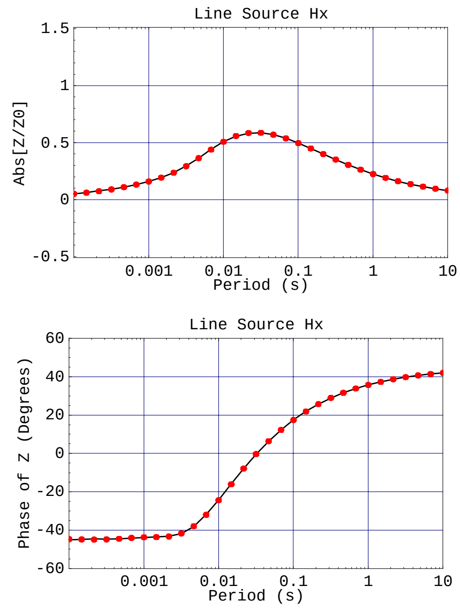

Figura 2. The red dots represent the calculated values and the black curve the exact mutual coupling ratio.

Example 3:

In this example we compare the calculated against the exact values of the mutual coupling ratio of the in-line coponent of the electrical field at 1000 m from an horizontal electrical dipole on an homogeneous 100 half-space.

$$Z/Z_0 = -\frac{\bar{x}^2}{2}\left[\int_0^\infty \frac{u(g+\bar{u})-2i}{g+\bar{u}}J_1(g\bar{x})\,dg-\bar{x}\int_0^\infty g\bar{u}J_0(g\bar{x})\,dg\right],$$

$$Z/Z_0 = \frac{1}{2}\left\{1+\left[1+\bar{x}(1+i)\right]e^{-\bar{x}(1+i)}\right\}$$

where J_1 is the Bessel function of order 1. The normalized distance $\bar{x}=x/\delta$, where $\delta=\sqrt{T/(\pi\mu_0\sigma)}$ is the skin depth and T is the period.

The Figure 3 shows the perfect adjustment between the calculated – formula 2 with J_0 and J_1 Hankel filters of Tables III and IV -- and the exact values of the mutual coupling ratio of the in-line component of the electrical field.

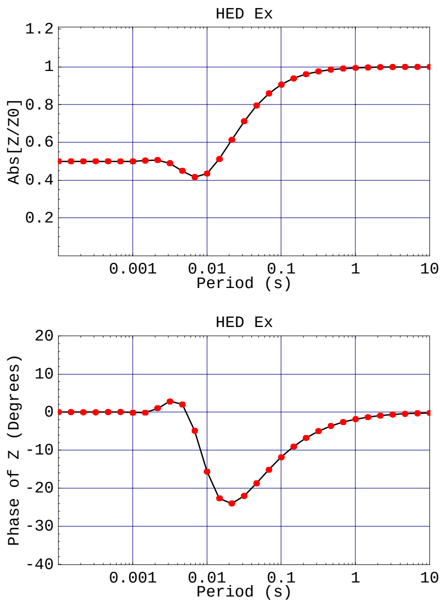

Figura 3. The red dots represent the calculated values and the black curve the exact mutual coupling ratio.

Conclusions

Despite their simplicity, the three examples shown above are typical for calculating sine, co-sine, J_0 and J_1 Hankel transforms in electrical geophysics. The kernels of the integrals in these three examples are very simple, as usual in one-dimensional layered earth. For the two-dimensional earth with three-dimensional source, the so-called 2.5 dimensional problems, the kernel for the sine and co-sine transforms are not so simple because they are calculated by numerical intensive methods (finite elements or integral equations). Thus, in this case it is desirable to have short optimized filters in order to minimize computer time.
Another reason for necessity of short optimized filters for calculating sine, co-sine, J_0 and J_1 Hankel transforms is that a large number of these integral transforms need to be calculated during the iterative inverse process of electrical geophysics data.
The filters coefficients shown in the Table I, II, II and IV, calculated by an automatic process adapted from Gupsarm and Sinha (1982) algorithm, can be a good alternative for much longer filter published in the literature.

Table I Co-sine filter

	Abscissas η_n	Coefficients W_n
1	-1.29915198386733D+01	0.00000446707672D+00
2	-1.24272709071081D+01	-0.00000272540914D+00
3	-1.18630219755430D+01	0.00000995316556D+00
4	-1.12987730439779D+01	0.00000003593369D+00
5	-1.07345241124127D+01	0.00002103641820D+00
6	-1.01702751808476D+01	0.00000948929254D+00
7	-9.60602624928244D+00	0.00005596897838D+00
8	-9.04177731771730D+00	0.00003907762436D+00
9	-8.47752838615216D+00	0.00016086940614D+00
10	-7.91327945458702D+00	0.00013776259357D+00
11	-7.34903052302188D+00	0.00047181234722D+00
12	-6.78478159145674D+00	0.00046523996184D+00
13	-6.22053265989160D+00	0.00139639635447D+00
14	-5.65628372832646D+00	0.00153610802958D+00
15	-5.09203479676132D+00	0.00416069317969D+00
16	-4.52778586519618D+00	0.00499470705662D+00
17	-3.96353693363104D+00	0.01246692217577D+00
18	-3.39928800206590D+00	0.01605195680795D+00
19	-2.83503907050076D+00	0.03749550612141D+00
20	-2.27079013893562D+00	0.05090885102758D+00
21	-1.70654120737048D+00	0.11190145021972D+00
22	-1.14229227580534D+00	0.15319049527128D+00
23	-0.57804334424020D+00	0.29619202597073D+00
24	-0.01379441267506D+00	0.26314282472466D+00
25	0.55045451889008D+00	-0.09973014459881D+00
26	1.11470345045522D+00	-1.72412432052151D+00
27	1.67895238202036D+00	1.11514563105521D+00
28	2.24320131358550D+00	-0.29772771117139D+00
29	2.80745024515064D+00	0.06144868733678D+00
30	3.37169917671578D+00	-0.01015050918409D+00

Table II Sine filter

	Abscissas η_n	Coefficients W_n
1	-6.60301637388159D+00	0.00000375466945D+00
2	-6.21433389656287D+00	-0.00000586160902D+00
3	-5.82565141924415D+00	0.00001507414780D+00
4	-5.43696894192542D+00	-0.00000751748112D+00
5	-5.04828646460670D+00	0.00003335640337D+00
6	-4.65960398728798D+00	0.00001458779557D+00
7	-4.27092150996925D+00	0.00010127733359D+00
8	-3.88223903265053D+00	0.00012980232894D+00
9	-3.49355655533180D+00	0.00041207401814D+00
10	-3.10487407801308D+00	0.00069605527643D+00
11	-2.71619160069436D+00	0.00183831543287D+00
12	-2.32750912337563D+00	0.00345717740224D+00
13	-1.93882664605691D+00	0.00841473994965D+00
14	-1.55014416873819D+00	0.01669978294703D+00
15	-1.16146169141946D+00	0.03861280203901D+00
16	-0.77277921410074D+00	0.07800177527823D+00
17	-0.38409673678201D+00	0.16998098262565D+00
18	0.00458574053671D+00	0.32396687801731D+00
19	0.39326821785543D+00	0.58277749001326D+00
20	0.78195069517416D+00	0.68051735467895D+00
21	1.17063317249288D+00	-0.09140093526035D+00
22	1.55931564981160D+00	-1.80579146705436D+00
23	1.94799812713033D+00	1.37727057650806D+00
24	2.33668060444905D+00	-0.48687474543221D+00
25	2.72536308176777D+00	0.12564244413231D+00
26	3.11404555908650D+00	-0.03051277822054D+00
27	3.50272803640522D+00	0.00740461871508D+00
28	3.89141051372395D+00	-0.00166171911043D+00
29	4.28009299104267D+00	0.00029263099338D+00
30	4.66877546836139D+00	-0.00002855156604D+00

Tabela III J_0 Hankel filter

	Abscissa	Coefficients
1	-8.79154501155931D+00	0.00238335617914D+00
2	-8.44755771427001D+00	-0.00923451277729D+00
3	-8.10357041698071D+00	0.02079895052544D+00
4	-7.75958311969141D+00	-0.03338702409972D+00
5	-7.41559582240211D+00	0.04477739890139D+00
6	-7.07160852511281D+00	-0.05167765846960D+00
7	-6.72762122782351D+00	0.05587472556026D+00
8	-6.38363393053421D+00	-0.05512276066568D+00
9	-6.03964663324491D+00	0.05444557860139D+00
10	-5.69565933595561D+00	-0.04892210690497D+00
11	-5.35167203866632D+00	0.04732656195005D+00
12	-5.00768474137702D+00	-0.03860491533605D+00
13	-4.66369744408772D+00	0.03920960657489D+00
14	-4.31971014679842D+00	-0.02644804816704D+00
15	-3.97572284950912D+00	0.03260982461445D+00
16	-3.63173555221982D+00	-0.01228397713755D+00
17	-3.28774825493052D+00	0.02956411797486D+00
18	-2.94376095764122D+00	0.00595004660943D+00
19	-2.59977366035192D+00	0.03317515498364D+00
20	-2.25578636306262D+00	0.03274470853033D+00
21	-1.91179906577332D+00	0.04933875502497D+00
22	-1.56781176848402D+00	0.07661759525931D+00
23	-1.22382447119472D+00	0.08883650000582D+00
24	-0.87983717390542D+00	0.15133386760606D+00
25	-0.53584987661612D+00	0.16507829454944D+00
26	-0.19186257932683D+00	0.26169301627952D+00
27	0.15212471796247D+00	0.24688255898384D+00
28	0.49611201525178D+00	0.27750176445175D+00
29	0.84009931254107D+00	-0.00155554395068D+00
30	1.18408660983037D+00	-0.33630611758063D+00
31	1.52807390711967D+00	-0.50651480451307D+00
32	1.87206120440897D+00	0.59211451923489D+00
33	2.21604850169827D+00	-0.23450184447820D+00
34	2.56003579898757D+00	0.05446237320377D+00
35	2.90402309627687D+00	-0.00928958955398D+00
36	3.2480103935661&D+00	0.00119894072586D+00
37	3.59199769085547D+00	-0.00008971645558D+00

Table IV J_1 Hankel filter

	Abscissas η_n	Coefficients W_n
1	-4.61195591517857D+00	0.00022403915103D+00
2	-4.27906647389069D+00	-0.00063831184603D+00
3	-3.94617703260281D+00	0.00113167818280D+00
4	-3.61328759131493D+00	-0.00081481684918D+00
5	-3.28039815002705D+00	0.00065948253261D+00
6	-2.94750870873917D+00	0.00015110345657D+00
7	-2.61461926745129D+00	0.00165282210988D+00
8	-2.28172982616341D+00	0.00080418132518D+00
9	-1.94884038487553D+00	0.00380611316285D+00
10	-1.61595094358765D+00	0.00619808024688D+00
11	-1.28306150229977D+00	0.01404440767965D+00
12	-0.95017206101189D+00	0.02189018716297D+00
13	-0.61728261972401D+00	0.04964931228922D+00
14	-0.28439317843613D+00	0.08370610919229D+00
15	0.04849626285175D+00	0.16660930791854D+00
16	0.38138570413963D+00	0.25725196330244D+00
17	0.71427514542751D+00	0.40730714915038D+00
18	1.04716458671539D+00	0.34895491488489D+00
19	1.38005402800327D+00	-0.04241399715350D+00
20	1.71294346929115D+00	-0.65781916295135D+00
21	2.04583291057903D+00	0.46094644953685D+00
22	2.37872235186691D+00	-0.15431387506167D+00
23	2.71161179315479D+00	0.03858981403104D+00
24	3.04450123444267D+00	-0.00949545480093D+00
25	3.37739067573055D+00	0.00231033358900D+00
26	3.71028011701843D+00	-0.00043488073049D+00
27	4.04316955830631D+00	0.00004191435466D+00

Acknowledgment

We wish to thank the agencies CNPq, CAPES and ANP for funding the PROEM (Laboratory for EM processing of the Department of Geophysics - UFPA),where this work was realized.

References

ANDERSON, W. L., 1979: Numerical integration of related Hankel transform of order o and 1 by adaptive digital filtering. Geophysics, 44: 1287-1305

DAS U. C. & GHOSH D. P., 1974. The determination of filter coefficients for the computation of standard curves for dipole resistivity sounding over layered earth by digital linear filtering. Geophysical Prospecting, 22: 765-780.

GHOSH, D. P., 1971, The application of linear filter theory to the direct interpretation of geo-electrical resistivity sounding measurements. Geophysical Prospecting, 19: 192-217.

GUPTASARMA, D., 1982. Optimization of short digital linear filters for increase accuracy. Geophysical Prospecting, 19: 192-217.

GUPTASARMA, D. & SINGH H., 1997. New digital filters for Hankel J and J Transforms. Geophysical Prospecting, 45: 745-762.

JOHANSEN, H. K. & SORENSEN, K., 1979. Fast Hankel Transforms. . Geophysical Prospecting, 27: 876-901.

KOEFOED, O. 1972, A note on the linear filter method of interpreting resistivity sounding data. Geophysical Prospecting, 20: 403-405.

KOEFOED, O. & DIRKS F. J. 1979. Determination of resistivity sounding filters by the Wiener-Hopf least squared method. Geophysical Prospecting, 27: 245-250.

KOEFOED, O. 1972, A note on the linear filter method of interpreting resistivity sounding data. Geophysical Prospecting, 20: 403-405.

MOHSEN, A. A. & HASHISH, E. A., 1994. The fast Hankel Transform. . Geophysical Prospecting, 42: 131-139.

NISSEN, J. & ENMARK, T., 1986. An optimized digital filter for Fourier transform. Geophysical Prospecting, 34: 897-903.

RIJO l. 1993. An optimized digital filter for the co-sine transform. Revista Brasileira de Geofísica: 10, 7-20.

RIJO L. Comment on “The fast Hankel Transform” by A. Mohdsen and E. Heshish. Geophysical Prospecting, 44: 473-477.

VERMA, R. K., 1977, Detectability by electromagnetic sounding system. IEEE Trans. Geosdi. Elect. GE – 15: 232-251.